PROCEEDINGS OF SCIENCE

Recent progress of the RD50 Collaboration – Development of radiation tolerant tracking detectors

A.Affolder[1], A.Aleev[2], P.P.Allport[1], L.Andricek[3], M.Artuso[4], L.Barabash[5], T.Barber[6], A.Barcz[7], M.R.Bartosik[8], M.Baselga[9], R.Bates[10], M.Battaglia[11], V.Benitez[9], J.Bernardini[12], C.Betancourt[6], A.Bhardwaj[13], G.M.Bilei[14], A.Blue[10], J.Bohm[15], M.Bomben[16], A.Borgia[4], L.Borrello[12], M.J.Bosma[17], T.J.V.Bowcock[1], J.Broz[18], M.Bruzzi[19], A.Brzozowski[20], P.Buhmann[21], C.Buttar[10], G.Calderini[16], M.Carna[15], N.Cartiglia[22], G.Casse[*1], M.Centis-Vignali[21], S.Charron[23], J.Chauveau[16], D.Chren[24], S.Cihangir[25], V.Cindro[26], P.Collins[8], E.Cortina Gil[27], D.Creanza[28], F.Crescioli[16], R.Dalal[13], W.de Boer[29], M.De Palma[28], P.Dervan[1], A.Dierlamm[29], D.Dobos[8], F.Doherty[10], I.Dolenc Kittelmann[8], Z.Dolezal[18], A.Dolgolenko[5], E.Donegani[21], A.Driewer[6], S.Dutta[12], R.Eber[29], D.Eckstein[30], T.Eichhorn[30], L.Eklund[10], I.Eremin[31], V.Eremin[31], J.Erfle[21], S.Esteban[9], N.Fadeeva[31], V.Fadeyev[11], S.Feigl[8], M.Fernandez[32], F.Fiori[12], N.Flaschel[30], C.Fleta[9], E.Focardi[19], D.Forshaw[1], E.Fretwurst[21], A.G Bates[10], M.Gabrysch[8], C.Gallrapp[8], C.Garcia[33], E.Garutti[21], E.Gaubas[34], M.-H.Genest[23], S.Gibson[8], M.Glaser[8], C.Goessling[35], M.Golovleva[36], A.Golubev[2], G.Gomez [32], I.Gorelov[37], V.Greco[9], G.Grégoire[27], I.Gregor[30], E.Grigoriev[2], A. A.Grillo[11], S.Grinstein[38], A.Groza[5], J.Guskov[39], J.Härkönen[40], F.G.Hartjes[17], F.Hartmann[29], S.Hidalgo[9], M.Hoeferkamp[37], R.Horisberger[41], A.Houdayer[23], D.Hynds[10], A. G.Ibanescu[42], I.Ilyashenko[31], R.Jaramillo[32], J.Jelena[3], J.Jentzsch[8], T.Jindra[18], A.Junkes[21], V.Kalendra[34], P.Kaminski[20], A.Karpenko[5], K.Kaska[8], N.Kazuchits [43], V.Kazukauskas[34], V.Khivrich[5], J.Kierstead[44], R.Klanner[21], R.Klingenberg[35], P.Kodys[18], E.Koffeman[17], Z.Kohout[24], A.Konoplyannikov[2], I.Korolkov[38], R.Kozlowski[20], M.Kozubal[20], G.Kramberger[26], S.Kuehn[6], S.Kwan[25], A.La Rosa[8], C.Lacasta[33], J.Lange[38], V.Lastovetsky[5], I.Lazanu[45], S.Lazanu[42], C.Lebel[23], G.Lefeuvre[4], V.Lemaitre[27], C.Leroy[23], Z.Li[44], G.Lindström[21], P.Litovchenko[5], I.Lopez[38], D.Loukas[46], M.Lozano[9], Z.Luczynski[20], P.Luukka[40], A.Macchiolo[47], A.Macraighne[10], T.Mäenpää[40], L.F.Makarenko[43], I.Mandić[26], D.Maneuski[10], N.Manna[28], G.Marchiori[16], R.Marco[33], S.Marti-Garcia[33], S.Marunko[39], P.Masek[24], M.Matysek[21], H.McDuff[37], A.Mekys[34], A.Messineo[12], M.Mikestikova[15], M.Mikuž[26], O.Militaru[27], M.Milovanovic[26], M.Moll[†8], R.Mori[6], H.-G.Moser[47], D.Muenstermann[8], F. J.Munoz Sanchez[32], A.Naletko[31], H.Neugebauer[8], A.Nikitin[2], R.Nisius[47], L. C.Nistor[42], S. V.Nistor[42], A.Nürnberg[29], A.Oblakowska-Mucha[48], Th.Ortlepp[49], V.OShea[10], N.Pacifico[8], C.Parkes[10], U.Parzefall[6], D.Passeri[14], M.Pawlowski[20], G.Pellegrini[9], H.Pernegger[8], M.Petasecca[14], G.U.Pignatel[14], I.Pintilie[42], L.Pintilie[42], K.Piotrzkowski[27], R.Plackett[10], J.Poehlsen[21], Th.Poehlsen[21], L.Polivtsev[5], J.Popule[15], S.Pospisil[24], M.Printz[29], D.Quirion[9], V.Radicci[41], R.Radu[42], K.Ranjan[13], R.Richter[3], J.Rodriguez[9], R.Roeder[49], S.Rogozhkin[2], T.Rohe[41], I.Rubinskiy[30], A.Rummler[35], A.Ruzin[39], H.F.W.Sadrozinski[11], M.Scaringella[19], B.Schumm[11], S.Seidel[37], A.Seiden[11], R.K.Shivpuri[13], P.Sicho[15], S.Singh[13], T.Slavicek[24], M.Solar[24], U.Soldevila-Serrano[33], V.Sopko[24], B.Sopko[24], N.Spencer[11], L.Spiegel[25], G.Steinbrueck[21], G.Stewart[10], J.Storasta[34], B.Surma[20], T.Szumlak[48], K.Tackmann[30], P.Tan[25], S.Terzo[47], T.Timo[40], M.Tomasek[15], K.Toms[37], S.Tsiskaridze[38], Yu.Tuboltsev[31], E.Tuominen[40], E.Tuovinen[40], T.Tuuva[36], M.Tylchin[39], H.Uebersee[49], M.Ullán[9], J.V.Vaitkus[34], M.van Beuzekom[17], E.Verbitskaya[31], I.Vila Alvarez[32], J.Visser[17], J.Vossebeld[1], V.Vrba[15], R.Wang[37], P.Weigell[47], L.Wiik[6], I.Wilhelm[18], T.Wittig[49], S.Wonsak[1], R.Wunstorf[35], M.Wysokinski[48], E.Yildirim[30], A.Zaluzhnyy[2], M.Zavrtanik[26], J.Zelazko[20], Z.Zhou[4], D.Zontar[26]

 http://pos.sissa.it/

PoS(Vertex 2013)026

PROCEEDINGS OF SCIENCE

[1] Department of Physics, University of Liverpool, United Kingdom
[2] State Scientific Center of Russian Federation, Institute for Theoretical and Experimental Physics, Moscow, Russia
[3] Semiconductor Laboratory of the Max-Planck-Society, Munich, Germany
[4] Experimental Particle Physics Group, Syracuse University, Syracuse, USA
[5] Institute for Nuclear Research of the Academy of Sciences of Ukraine, Radiation PhysicDepartments
[6] University of Freiburg
[7] Institute of Electronics Technology/ Institute of Physics PAS, Warsaw, Poland
[8] CERN, Geneva, Switzerland
[9] Centro Nacional de Microelectrónica (IMB-CNM, CSIC), Barcelona, Spain
[10] Dept. of Physics & Astronomy, Glasgow University, Glasgow, UK
[11] Santa Cruz Institute for Particle Physics
[12] Universita‘ di Pisa and INFN sez. di Pisa, Italy
[13] Center for Detector and Related Software Technologies, Department of Physics & Astrophysics, University of Delhi, India
[14] I.N.F.N. and Università di Perugia - Italy
[15] Institute of Physics, Academy of Sciences of the Czech Republic, Praha, Czech Republic
[16] Laboratoire de Physique Nucléaire et de Hautes Energies, UPMC and Université Paris-Diderot and CNRS/IN2P3, Paris, France
[17] National Institute for Subatomic Physics (Nikhef), Amsterdam, The Netherlands
[18] Charles University Prague, Czech Republic
[19] INFN Florence - Department of Energetics, University of Florence, Italy
[20] Institute of Electronic Materials Technology, Warszawa, Poland
[21] Institute for Experimental Physics, University of Hamburg, Germany
[22] INFN Torino, Torino
[23] Groupe de la Physique des Particules, Université de Montreal, Canada
[24] Czech Technical University in Prague, Czech Republic
[25] Fermilab, USA
[26] Jožef Stefan Institute and Department of Physics, University of Ljubljana, Ljubljana, Slovenia
[27] Université catholique de Louvain, Institut de Physique Nucléaire, Louvain-la-Neuve, Belgium
[28] Dipartimento Interateneo di Fisica & INFN - Bari, Italy
[29] Karlsruhe Institute of Technology, Institut für Experimentelle Kernphysik, Karlsruhe, Germany
[30] Deutsches Elektronen Synchrotron
[31] Ioffe Physical-Technical Institute of Russian Academy of Sciences, St. Petersburg, Russia
[32] Instituto de Fisica de Cantabria (CSIC-UC)
[33] IFIC, joint research institute of CSIC and Universitat de Valencia-Estudi General, Valencia, Spain
[34] Institute of Materials Science and Applied Research, Vilnius University, Vilnius, Lithuania
[35] Technische Universitaet Dortmund, Lehrstuhl Experimentelle Physik IV, Dortmund, Germany
[36] Lappeenranta University of Technology, Lappeenranta, Finland
[37] Department of Physics and Astronomy, University of New Mexico, Albuquerque, NM, USA
[38] Institut de Física dAltes Energies (IFAE),Bellaterra (Barcelona), Spain
[39] Tel Aviv University, Israel
[40] Helsinki Institute of Physics, Helsinki, Finland
[41] Paul Scherrer Institut, Laboratory for Particle Physics, Villigen, Switzerland
[42] National Institute for Materials Physics, Bucharest - Magurele, Romania
[43] Belarusian State University, Minsk
[44] Brookhaven National Laboratory, Upton, NY, USA
[45] University of Bucharest, Faculty of Physics
[46] NCSR Demokritos, Greece
[47] Max-Planck-Institut fuer Physik, Munich, Germany
[48] AGH - University of Science and Technology, Faculty of Physics and Applied Computer Science, Krakow, Poland
[49] CiS Forschungsinstitut fürMikrosensorik und Photovoltaik GmbH, Erfurt, Germany

The CERN RD50 Collaboration "Radiation hard semiconductor devices for high luminosity colliders" is undertaking a massive R&D programme across High Energy Physics (HEP) Experiments boundaries to develop silicon sensors with increased radiation tolerance. Highest priority is to provide concepts and prototypes of high performance silicon sensors for the High-Luminosity Large Hadron Collider (HL-LHC) Experiments at CERN and other future HEP Experiments operating in severe radiation environments. This paper gives an overview of the RD50 collaboration activities and describes some examples of recent developments. Emphasis is put on the characterization of microscopic radiation induced defects and their impact on the sensor performance, the evaluation and parametrization of electric fields inside irradiated sensors, progress in device modeling using TCAD tools, the use of p-type silicon as strip and pixel sensor material and finally the first steps towards the exploitation of impact ionization (*charge multiplication*) in irradiated sensors.

22nd International Workshop on Vertex Detectors,
15-20 September 2013
Lake Starnberg, Germany

1. Introduction

The upgrade of the LHC towards the HL-LHC [1] with increased luminosity is envisaged for the years 2023 to 2025. Unprecedented radiation levels will be reached for the inner tracking detectors which correspond to about $2 \times 10^{16} n_{eq} cm^{-2}$ for the inner pixel layers and $1 \times 10^{15} n_{eq} cm^{-2}$ for the innermost strip sensor layers when the anticipated integrated Luminosity of $3000 fb^{-1}$ has been reached. RD50 is an international collaboration with 49 participating institutes and 270 members, working on the development of radiation tolerant semiconductor sensors for such high radiation environments [2]. A very comprehensive research program is undertaken by RD50. It starts with the characterization of radiation induced microscopic defects, includes mitigation approaches based on material and device engineering as well as device geometry optimization studies and finally ends with the use of presently available high speed electronic readout chips to characterize sensor performance under most realistic conditions. In all these activities a very close link is kept with the corresponding R&D activities in the HEP Experiments. In the following some recent results are presented that represent only part of the overall work program.

2. Defect Characterization

The major source for the radiation induced degradation of silicon sensor performance is the formation of microscopic defects in the semiconductor crystal bulk of the device. Extensive work has been performed over recent years within the RD50 community to identify the defects that cause the various degradation phenomena on the sensor level [3]. The most relevant defects are listed in Table 1. It was for example shown that the defects H(116K), H(140K) and H(152K) are responsible for the so-called *reverse annealing*, while the defect E(30K) and BD play a major role in the production of positive space charge during irradiation. The latter are the reason why differences in the effective doping concentration N_{eff} are observed on the one hand between proton and neutron irradiated silicon detectors and on the other hand between oxygen rich and oxygen lean silicon materials. Finally the defects E4 and E5 are the main reason for the high leakage current after hadron irradiation, while the defect I_p contributes with negative space charge and leakage current and is relevant after gamma and low energy electron irradiation. Recently, focus was given to the question as to which electron energy is needed to produce extended defects (*clusters*) in silicon [8]. Figure 1 gives an example of this work. Detectors made from different silicon materials have been exposed to electrons with energies between 1.5 and 15 MeV and investigated by means of TSC (Thermally Stimulated Current) and other methods. It was found that for 1.5 MeV electrons only point defects were produced, while for an electron energies of 3.5 MeV and above extended defects identical to those observed after hadron irradiation become visible. Identical to the situation in hadron irradiated silicon, these extended defects do not show a dependence on the oxygen content of the material as is shown in Figure 1(b) on the example of the H-defects responsible for the *reverse annealing*. The oxygen related point defects, like the E(30K) defect, depend as expected on the oxygen content of the material. The ratio of point defects like VO towards the higher order defects like V_2 and V_3 could be determined as function of electron energy. The resulting data and the

*Co-spokesperson
†Co-spokesperson, speaker and corresponding author. Email: michael.moll@cern.ch

Defect	$\sigma_{n,p}[cm^2]$	$E_A[eV]$	Assignment and impact on sensor
E(30K)	$\sigma_n = 2.3 \times 10^{-14}$	$E_C - 0.1$	Electron trap with donor level in upper half of bandgap; generates positive spacecharge; higher generation in oxygen rich material; higher generation after proton than after neutron irradiation [4].
$BD_A^{(0/++)}$ $BD_B^{(+/++)}$	$\sigma_n = 2.3 \times 10^{-14}$ $\sigma_n = 2.7 \times 10^{-12}$	$E_C - 0.225$ $E_C - 0.15$	Bistable Thermal Double Donor TDD2; electron trap with donor levels in the upper half of bandgap; introducing positive spacecharge; strongly produced in oxygen rich material [5].
$I_p^{(+/0)}$ $I_p^{(0/-)}$	$\sigma_p = (0.5-9) \times 10^{-15}$ $\sigma_n = 1.7 \times 10^{-15}$ $\sigma_p = 9 \times 10^{-14}$	$E_V - 0.23$ $E_C - 0.55$	V_2O or carbon related defect with donor and acceptor level; introducing negative spacecharge and leakage current; strongly generated in oxygen lean material [4].
$E4$ $E5$	$\sigma_n = 1 \times 10^{-15}$ $\sigma_n = 7.8 \times 10^{-15}$	$E_C - 0.38$ $E_C - 0.46$	Acceptor levels assigned to the double and single charged acceptor states of V_3; generating leakage current [6].
$H(116K)$ $H(140K)$ $H(152K)$	$\sigma_p = 4.0 \times 10^{-14}$ $\sigma_p = 2.5 \times 10^{-15}$ $\sigma_p = 2.3 \times 10^{-14}$	$E_V + 0.33$ $E_V + 0.36$ $E_V + 0.42$	Acceptor levels; extended defects (clusters of interstitials or vacancies); introducing negative spacecharge [7].

Table 1: List of radiation induced defect levels with a major impact on silicon sensor performance. Given are the defect labels, the cross sections σ_n and σ_p for electrons and holes, the energy level in the band gap E_A with respect to either the conduction (E_C) or the valance (E_V) band and a very brief description of the impact on the sensor.

fact that the leakage current Non-Ionizing-Energy-Loss (NIEL) scaling is much better explained by an *effective NIEL* [9] than by the *classical NIEL* hypothesis gives rise to further work in order to improve the NIEL scaling approach for all damage calculations.

3. Device Simulations

With the growing knowledge on the defects responsible for the radiation induced sensor degradation and the availability of sophisticated commercial TCAD device simulation tools, simulations are rising in importance to study, understand and predict radiation damage effects in silicon devices. The impact of several radiation induced defect levels as well as e.g. impact ionization effects in high field regions or the importance of radiation induced changes of the oxide charge densities can accurately be modeled without the need to study the mathematical background of finite element modeling. Within RD50 a working group on device simulations was recently formed to exploit this technique. In a first step simulations of the *double junction effect* [10] were performed on the basis of existing defect models to compare the various simulation tools and form a common ground for further studies. TCAD simulations have meanwhile been performed that can reproduce various experimental results on irradiated sensors like Transient Current Technique (TCT) [11] and edge-TCT [12] measurements, Charge Collection Efficiency (CCE) data obtained in test-beams [13], avalanche effects in highly damaged devices [14], isolation and breakdown effects close to

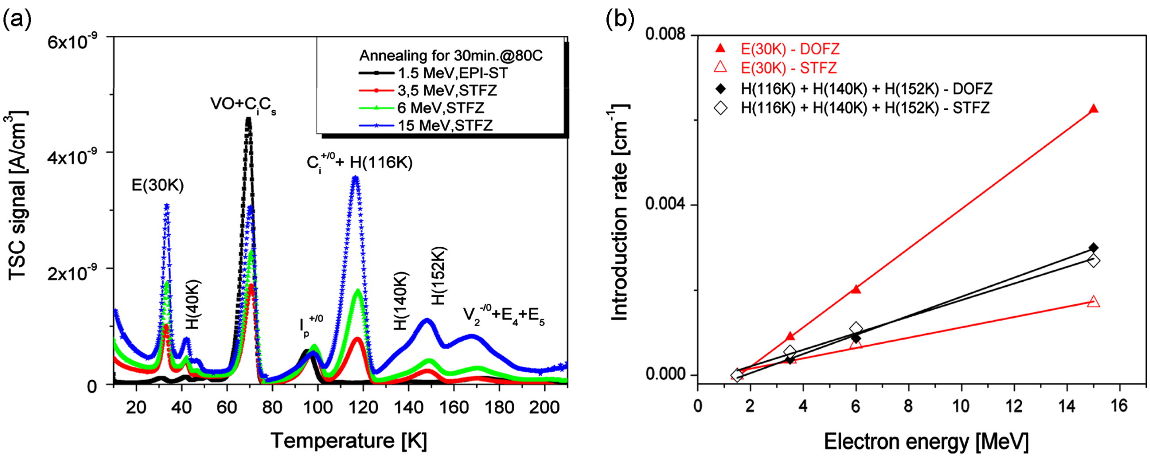

Figure 1: (a) TSC spectra for different electron energies measured on EPI-ST (1.5 MeV) and STFZ materials (3.5, 6, and 15 MeV) after annealing for 30 min at 80°C, scaled to a fluence of $\phi = 6 \times 10^{14} cm^{-2}$, and (b) introduction rate for E(30K) and H defects versus electron kinetic energy, after annealing for 30 min at 80°C in STFZ and DOFZ materials [8].

the device surface [15] and even Lorentz Angle shifts [16]. However, there is still a wide variety of parameter sets used to represent the radiation induced defect levels and a lack in consistency between measured defect data and parameters used in the simulations. The RD50 simulation working group is aware of these challenges and making good progress towards more consistent simulation input parameters. It can be rightfully stated that TCAD simulations are gaining in importance for the understanding of radiation damage and start to get predictive power for the performance of irradiated devices.

4. Characterization and Parametrization of the Electric Field

A lot of work has been invested in the parametrization of the effective space charge N_{eff} as function of particle fluence, annealing time and silicon material (see e.g. [17]). Usually this parameter is obtained by extracting the depletion voltage V_{dep} from a CV characteristics of the detector assuming a constant space charge within the sensor. However, TCT measurements have shown that this assumption is not valid and that the electric field shape within the sensor can be relatively complex. It would therefore be very profitable to have a parameterization of the electric field within the device. In combination with adequate trapping time parameterizations and the weighting field of the device under study more accuracy could be gained in predicting the charge collection efficiency and the sensor performance after irradiation.
With the introduction of *edge-TCT* [18] the characterization of the electric field in irradiated sensors has taken a substantial step forward. In this technique a narrow pulsed infrared laser beam is scanned over the side (edge) of a segmented detector. In this way electron-hole pairs are created almost uniformly along the beam in a fixed depth of the sensor. The recorded TCT pulses as function of depth in the device can then be used to extract the sum of the electron and hole carrier velocities from the risetime of the TCT pulse. Examples of such depth scans for an irradiated p-

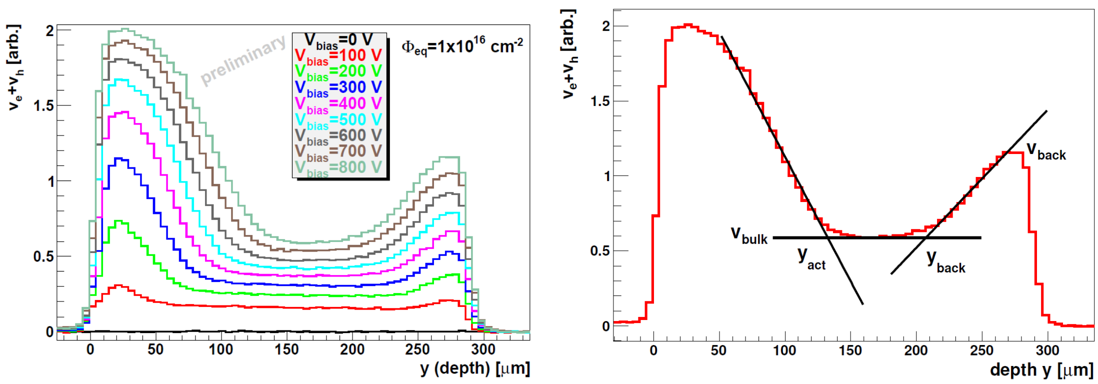

(a) (b)

Figure 2: (a) Velocity profiles at different bias voltages for a p-type detector irradiated with a neutron fluence of $10^{16} n_{eq} cm^{-2}$ and annealed for 80min at 60°C. (b) Example of the determination of model parameters for the parametrization of the velocity profile obtained at 800V [19].

type ministrip detector as function of bias voltage are shown in Figure 2(a). For this detector the *double-junction* effect is clearly visible indicating that the space charge is negative underneath the segmented front (n^+) electrode at $y = 0$, while the space charge close to the back (p^+) electrode is positive. The edge-TCT measurements have proven to be very useful for benchmarking TCAD device simulations. Furthermore, they allow a new way to parametrize radiation damage. Rather than to parametrize the depletion voltage of a device, the electric field (or more precisely the free carrier velocity profiles) can be parametrized. In a first approach, a simple model has been assumed to represent the electric field in the device [19]. The model is based on the assumption that a region with constant space charge is located underneath each of the two electrodes. One region with negative space charge, one with positive space charge. The corresponding shape of the electric field profile (respectively velocity profile) is represented in Figure 2(b). Between these two regions a neutral bulk with constant electric field is assumed. The lines indicated in the figure represent the parametrization of the drift velocity profile. Parameters are the drift velocities at the back and front electrode and within the bulk region as well as the start and the end of the neutral bulk region. Extending this parametrization over a wide fluence and irradiation particle type range (like previously done for N_{eff}) in combination with a proper weighting field and a standard trapping model will allow a more precise prediction of the detector performance versus fluence than present N_{eff} models can do [19].

5. Segmented sensors with readout on the n-implant (n-in-p and n-in-n sensors)

Within the RD50 collaboration n-in-p strip sensors[1] have been successfully developed and demonstrated to be more radiation tolerant than p-in-n sensors while offering at the same time an improved immunity against long-term room temperature annealing after high levels of irradiation (see e.g. [20]). These were the most convincing arguments that brought ATLAS and CMS to the

[1] n-in-p: n-type implants form the segmented front electrodes in p-type silicon

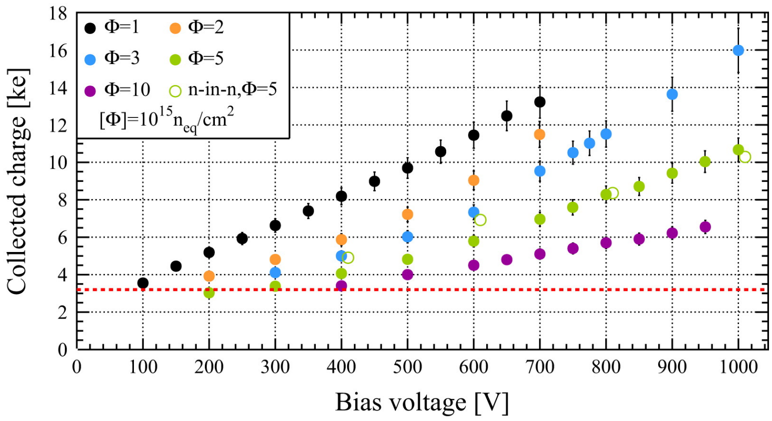

Figure 3: Collected Charge (MPV - Most Probable Value) for neutron irradiated n-in-p planar pixel sensor of 285 μm thickness. The measurements were performed with a beta-source (^{90}Sr) as a function of the bias voltage. The dotted red line indicates the tuned threshold of the sensors, 3.2 ke [22].

decision to make n-in-p sensors the baseline choice for their HL-LHC tracker upgrades.

In view of the significantly increased area to be covered with pixel sensors in the HL-LHC vertex detectors and the corresponding pressure to reduce cost, a development on n-in-p pixel sensors has been started (see e.g. [21]). Compared to the presently used n-in-n pixel sensor technology the n-in-p sensor technology is easier to produce and therefore less expensive, since a double-sided processing is not needed. Furthermore, the homogeneous backside of the n-in-p sensors is less problematic to handle, allows easier mounting of the sensors and enables easier wafer thinning methods. The latter are used to reduce the mass of the sensor and therefore the multiple scattering of particle in the inner tracking volume. The only potential drawback of this technology is the fact that spark protection has to be assured between the low potential of the readout chip and the edges of the sensor. However, feasible solutions have been developed and demonstrated to offer good protection up to more than 1000V. Prototypes of p-type pixel sensors have been produced, irradiated and successfully tested. As for n-in-n pixel sensors, it has been demonstrated that even after irradiation with a fluence of $10^{16} n_{eq} cm^{-2}$ enough charge is collected at the sensor electrode to produce a signal to noise ratio that allows for efficient particle tracking provided a sufficiently high voltage is applied [22]. Figure 3 gives an example of the signal measurements as function of applied voltage. P-type sensors are thus well suited to become a cost-effective sensor option for future radiation tolerant pixel detectors.

A question under study is the optimal thickness of the sensors, which impacts on the one hand on the material budget, but on the other hand also on the signal. Surprisingly, recent measurements have shown that after high levels of radiation thin detectors can deliver even higher signals than thick sensors. This is demonstrated in Figure 4 for n-in-p-type pixel sensors with different thickness. It can be seen that for sensors exposed to $2 \times 10^{15} n_{eq} cm^{-2}$ the optimal thickness is about 150 μm if 200-300 V are applied to the sensor. This striking result is originating from the fact that charge collection after extreme particle fluences is impacted by very strong charge trapping (charge loss) which reduces the advantage of thick sensors. Furthermore, thin sensors profit from the higher electric field strength at same voltage.

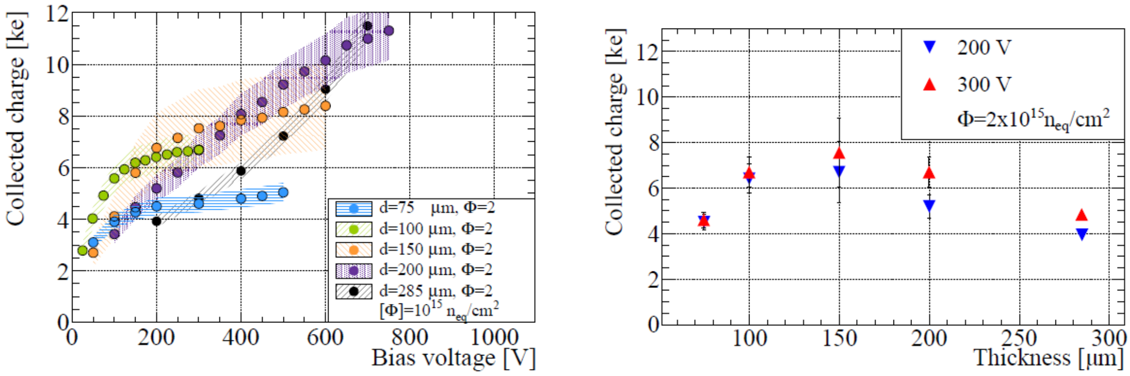

Figure 4: Comparison of collected charge as measured with a Sr^{90} source on irradiated ($\phi_{eq} = 2 \times 10^{15} n_{eq} cm^{-2}$) p-type pixel sensors with different thickness bump-bonded to ATLAS FEI4 readout chips [23]. Left: Collected charge as function of voltage. Right: Collected charge as function of device thickness for 200V and 300V.

6. Charge multiplication

The *charge multiplication effect* has been observed in several experiments on different irradiated detector types [24 – 27]. It was found that the signal produced by a minimum ionizing particle (mip) or a laser beam in a highly irradiated silicon sensor operated under high bias voltage was higher than expected and in some cases even higher than the signal obtained on an identical non-irradiated sensor. The reason is found in the electric field strength close to the n-in-p junction of the sensors which is high enough to accelerate electrons beyond the onset of impact ionization. A detailed explanation of this effect and its surprising stability in operating below the device breakdown has been given in device simulations [28]. RD50 has taken up the challenge to understand if the *charge multiplication effect* can be exploited to obtain a higher signal to noise ratio for irradiated sensors. Two approaches have been followed so far.

In a first attempt the properties of the n-p junction of strip sensors were modified by either changing the shape and concentration of the n^+ doping profile or by introducing a $5\mu m$ wide polysilicon filled trench with different depths in the middle of the strip implant [29]. However, while it could be clearly demonstrated that the junction engineering is a means to modify and tailor the multiplication effect there was a lack in understanding the systematics of the obtained results. For example, the collected charge did not scale in a systematic way with the depth of the trenches (see [29]). Further experimental and simulation work is therefore under way to gain a deeper understanding of the junction engineering approach.

In a second approach devices called *Low Gain Avalanche Detectors - LGAD* with an intrinsic gain factor of about 10 already before irradiation were produced [30]. The required high electric field is achieved with an additional p^+doping layer under the n^+ front electrode. The device structure is therefore very similar to the structure of an *Avalanche Photo Detector (APD)* operated in linear mode. Figure 5(a) shows a laser scan over the surface of a LGAD diode demonstrating a homogeneous gain of about 7 over the active area accessible to the laser beam [31]. First irradiation tests with neutrons [32] have unfortunately shown a loss of gain after irradiation. After a fluence

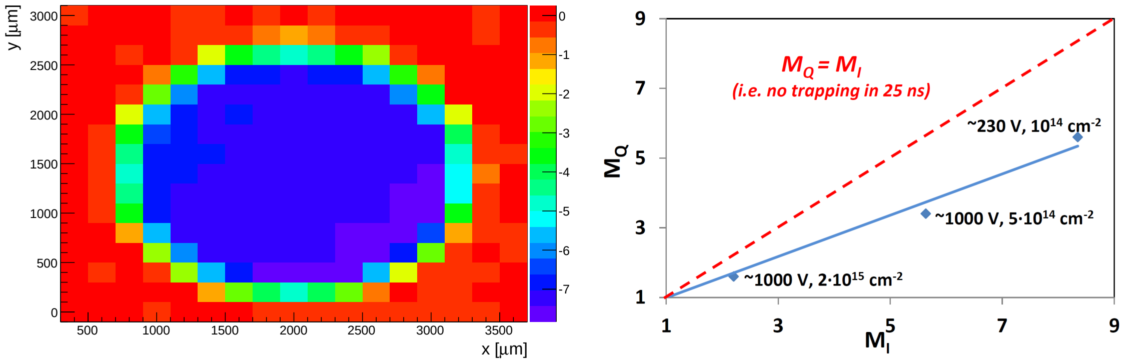

(a) (b)

Figure 5: (a) Laser scan over the surface of an LGAD diode structure. The color indicates the gain on the signal due to the amplification layer. The circular structure is the opening in the metal layer [31] (b) Multiplication factors (gain) for the obtained signal M_Q versus multiplication factor of the leakage current M_I for neutron irradiated LGAD diode structures. The neutron irradiation fluence and the voltage used for the measurements are indicated [32].

of $5 \times 10^{14} n_{eq} cm^{-2}$ the gain was reduced from about 7 to about 3. Some experimental results are shown in Figure 5(b) where the amplification of the radiation induced leakage current M_I is plotted against the gain in signal M_Q. Due to the charge trapping the amplification of the signal is smaller than the amplification of the leakage current, while without trapping $M_Q = M_I$ is expected as indicated by the red line in the figure. For each data point the neutron fluence is given in the figure demonstrating the decrease of M_Q with increasing fluence. Although the observed loss in gain is still under investigation, the most reasonable explanation seems to be that the Boron that is forming the p^+ amplification layer is removed (deactivated) due to radiation effects. With the loss of active boron the field strength in the amplification layer is decreasing and correspondingly the gain is reduced.

7. Summary

The RD50 collaboration has gained significant achievements in the understanding of radiation effects and the development of radiation tolerant silicon sensors. In this article recent progress in the characterization of microscopic radiation induced defects and their impact on the sensor performance, the evaluation and parametrization of electric fields inside irradiated sensors, progress in device modeling using TCAD tools, the use of p-type silicon as strip and pixel sensor material and finally the first steps towards the exploitation of impact ionization (*charge multiplication*) in irradiated sensors have been presented. Further very successful RD50 projects, like for example the development of sensors with slim edges or 3D sensors, the prediction of radiation damage for the LHC Experiments and the study of different silicon materials (EPI, MCZ, DOFZ, FZ) were not covered and can be found in other RD50 publications [2].

PoS(Vertex 2013)026

References

[1] Lucio Rossi and Oliver Brüning. High Luminosity Large Hadron Collider - A description for the European Strategy Preparatory Group. *CERN-ATS-2012-236*.

[2] The RD50 collaboration: http://www.cern.ch/rd50.

[3] A.Junkes. Status of defect investigations. *Proceedings of Science*, Vertex 2011(035), 2011.

[4] Ioana Pintilie et al. Radiation-induced point- and cluster-related defects with strong impact on damage properties of silicon detectors. *Nucl. Inst. and Meth. Phys. Res. A*, 611:52–68, 2009.

[5] E.Fretwurst et al. Radiation damage studies on MCz and standard and oxygen enriched epitaxial silicon devices. *Nucl. Inst. and Meth. Phys. Res. A*, 583(1):58–63, 2007.

[6] R.M.Fleming et al. Transformation kinetics of an intrinsic bistable defect in damaged silicon. *J.Appl.Phys.*, 111:023715, 2012.

[7] I.Pintilie et al. Cluster related hole traps with enhanced-field-emission - the source for long term annealing in hadron irradiated Si diodes. *Applied Physics Letters*, 92:024101, 2008.

[8] Roxana Radu et al. Radiation damage in n-type silicon diodes after electron irradiation with energies between 1.5 MeV and 15 MeV. *Nucl. Inst. and Meth. Phys. Res. A*, 730:84–90, 2013.

[9] C.Inguimbert et al. Effective NIEL in Silicon: Calculation Using Molecular Dynamics Simulation Results. *IEEE Transactions on Nuclear Science*, 57(4):1915–1923, 2010.

[10] V.Eremin et al. The origin of double peak electric field distribution in heavily irradiated silicon detectors. *Nucl. Inst. and Meth. Phys. Res. A*, 476(3):556–564, 2002.

[11] Robert Eber. Simulation of CV, TCT and CCE with an effective 2-defect model. *22^{nd} RD50 Workshop, June 2013*.

[12] Timo Peltola. Non-uniform 3-level defect model & status of edge-TCT simulations. *23^{rd} RD50 Workshop, November 2013*.

[13] Timo Peltola. Simulations of edge-TCT, interstrip resistance and 2-defect model CCE. *22^{nd} RD50 Workshop, June 2013*.

[14] E. Verbitskaya et al. Restriction on the gain in collected charge due to carrier avalanche multiplication in heavily irradiated Si strip detectors. *Nucl. Inst. and Meth. Phys. Res. A*, 730:66–72, 2013.

[15] Ranjeet Dalal. Simulations of Hadron Irradiated n+p- Si Strip Sensors Incorporating Bulk and Surface Damage. *23^{rd} RD50 Workshop, November 2013*.

[16] Andreas Nürnberg. T-CAD simulation of Lorentz angle. *23^{rd} RD50 Workshop, November 2013*.

[17] Michael Moll. *Radiation Damage in Silicon Particle Detectors - Microscopic Defects and Macroscopic Properties -. PhD thesis, University of Hamburg,*, 1999.

[18] G.Kramberger, V.Cindro, I.Mandić, M.Mikuž, M.Milovanović, M.Zavrtanik, K.Žagar. Investigation of Irradiated Silicon Detectors by Edge-TCT . *IEEE Transactions on Nuclear Science*, 57(4):2294–2302, 2010.

[19] Gregor Kramberger et al. Electric field modeling in heavily irradiated silicon detectors based on Edge-TCT measurements. *Proceedings of Science*, Vertex 2013(022), 2012.

[20] Gianluigi Casse. Radiation hardness of p-type silicon detectors. *Nucl. Inst. and Meth. Phys. Res. A*, 612:464–469, 2010.

[21] A.Macchiolo et al. Thin n-in-p pixel sensors and the SLID-ICV vertical integration technology for the ATLAS upgrade at the HL-LHC. *Nucl. Inst. and Meth. Phys. Res. A*, 731:210–215, 2013.

[22] Dean Forshaw. Recent results of the ATLAS upgrade Planar Pixel Sensors R&D project. *Nucl. Inst. and Meth. Phys. Res. A*, 730:44–49, 2013.

[23] S.Terzo. Irradiated n-in-p planar pixel sensors with different thicknesses and active edge designs. *23rd RD50 Workshop, November 2013*.

[24] G.Casse et al. Enhanced efficiency of segmented silicon detectors of different thicknesses after proton irradiations up to 1×1016 neq cm2. *Nucl. Inst. and Meth. Phys. Res. A*, 624:401–404, 2010.

[25] J.Lange et al. Properties of a radiation-induced charge multiplication region in epitaxial silicon diodes. *Nucl. Inst. and Meth. Phys. Res. A*, 622:49–58, 2010.

[26] I.Mandic et al. Observation of full charge collection efficiency in heavily irradiated n+p strip detectors irradiated up to 3×1015 neq/cm2. *Nucl. Inst. and Meth. Phys. Res. A*, 612:474–477, 2010.

[27] A.Affolder et al. Silicon detectors for the sLHC. *Nucl. Inst. and Meth. Phys. Res. A*, 658:11–16, 2010.

[28] V.Eremin et al. Avalanche effect in Si heavily irradiated detectors: Physical model and perspectives for application. *Nucl. Inst. and Meth. Phys. Res. A*, 658:145–151, 2011.

[29] G.Casse et al. Charge multiplication in irradiated segmented silicon detectors with special strip processing. *Nucl. Inst. and Meth. Phys. Res. A*, 699:9–13, 2013.

[30] G.Pellegrini et al. *Technology developments and first measurements of Low Gain Avalanche Detectors (LGAD) for High Energy Physics applications*. *submitted for publication in Nucl.Instr. and Meth. Phys. Res. A*.

[31] Marcos Fernández. *Thermal characterization of Low Gain Avalanche Diodes*. *23rd RD50 Workshop, November 2013*.

[32] G.Kramberger. Studies of CNM diodes with gain. *22nd RD50 Workshop, June 2013*.

PoS(Vertex 2013)026